Experimental rheometry of melts and supercooled liquids in the system NaAlSiO₄-SiO₂: Implications for structure and dynamics

Daniel J. Stein, Frank J. Spera

Institute for Crustal Studies and Department of Geological Sciences, University of California, Santa Barbara,
Santa Barbara, California 93106, U.S.A.

Abstract

Viscometric data for seven compositions in the system $NaAlSiO_4$-SiO_2 have been collected by the technique of concentric cylinder rheometry in the temperature and shear rate ranges 1000–1300 °C and 10^{-2}–8/s, respectively, for single-phase melts or supercooled liquids. As a function of increasing $NaAlSiO_4$ (N) content, the compositions include the tridymite + albite eutectic (N_{20}, eutectic I), the thermal divide composition (N_{33}, $NaAlSi_3O_8$), the albite + nepheline solid-solution eutectic (N_{41}, eutectic II), jadeite composition (N_{50}, $NaAlSi_2O_6$), and peritectic composition (N_{60}). The range of experimentally accessible shear rates is not large enough to evaluate fully the extent of pseudoplastic (non-Newtonian) behavior across the compositional spectrum. However, a small departure from Newtonian behavior is not excluded for some of the compositions. Measured viscosities vary from nearly 10^8 to 10^4 Pa·s for the range of compositions and temperatures investigated. Temperature-viscosity data are extremely well fitted by both Arrhenian (two-parameter) and Fulcher (three-parameter) expressions. In cases where the temperature range is large (e.g., $NaAlSi_3O_8$ and $NaAlSi_2O_6$ melts) the Fulcher fit is statistically significant. In the Fulcher fit, there is a systematic increase in T_0 (the Vogel temperature) indicative of increasing melt fragility as the concentration of $NaAlSiO_4$ component increases. Similarly, there is a linear relationship between Arrhenian activation energy (E_η) and the mole fraction of $NaAlSiO_4$ (X_N) according to the expression $E_\eta = (499 - 158)X_N$ (with E_η in kilojoules per mole), which is valid across the entire $NaAlSiO_4$-SiO_2 join. The increase in Vogel temperature and decrease in activation energy for viscous flow and isothermal viscosity as $NaAlSiO_4$ is added to molten silica may be rationalized microscopically on the basis of the increased Al-O bond length relative to Si-O, the reduction in bond energy for Al-O compared with Si-O, and the smaller mean TOT intertetrahedral bridging angle for Al-O-Si relative to Si-O-Si.

Introduction

Viscosity is among the most widely studied properties of silicate melts, with obvious relevance to the study of momentum transport phenomena in magmas, and includes implications for other processes such as chemical and tracer diffusion, advection of heat, and the nucleation and growth rates of solid or fluid phases in magmatic systems. For some time, there has existed an extensive body of viscosity measurements on silicate melts, supercooled liquids, and glasses, spanning a considerable range of temperatures and compositions of geochemical interest (e.g., Bottinga and Weill, 1972; Shaw, 1972; Urbain et al., 1982; Richet, 1984; Mysen, 1987, 1988). Experimental measurements of viscosity in molten silicates and silicate multiphase mixtures as a function of pressure, oxidation state, and deformation rate have become more common in the last decade (e.g., Kushiro, 1976, 1978; Dingwell and Virgo, 1987; Scarfe et al., 1987; Ryerson et al., 1988; Spera et al., 1988), although a great deal remains to be accomplished, especially for multiphase sys-

tems. At the most fundamental level, the complex relationship between the dynamics of a melt and its structure at the atomic scale must be understood in order to achieve a quantitative understanding of magmatic phenomena.

In order to organize the data available at the time, Bottinga and Weill (1972) and Shaw (1972) developed algorithms for calculating the viscosity of silicate melts, independent of shear rate, accurate to within a factor of 5 or less for a given temperature and composition in terms of oxide components at 100 kPa of total pressure. These strictly empirical models, although not based on analysis of any physical mechanism, are useful in estimating viscosities within the range of magmatic compositions and temperatures. It has been noted that logarithmic viscosity isotherms in simple binary and ternary systems of metal oxide and silica exhibit apparent linear variation with silica mole fraction within restricted compositional intervals; other properties show similar behavior. The boundaries of these intervals intersect invariant (e.g., eutectic) compositions on the equilibrium phase diagram of the system (Babcock, 1968; Urbain et al., 1982; see Spera et

al., 1988, their Table 2 for a summary). According to Urbain et al. (1982), this suggests that the phase transitions that occur along the liquidus reflect composition-dependent changes in liquid structure that persist far above the liquidus, resulting in the segmented linear dependence of the viscosity (see Figs. 2 and 8 in Urbain et al., 1982). As noted previously (Spera et al., 1988), this pattern is commonly observed in plots of log η vs. mean molecular weight for organic polymer fluids such as the linear chain polyisobutylenes. The book by Ferry (1980) documents many such examples. It is the correlation between microscopic structure and its projection into the macroscopic realm that guides our understanding of the liquid state (Hansen and McDonald, 1986; Ziman, 1979; Evans and Morriss, 1990; Scamehorn and Angell, 1991) and provides a formidable challenge to experimentalists and theoreticians alike.

Phase relations for the system $NaAlSiO_4$-SiO_2 ($NaAlSiO_4 = N_{100}$) at 100 kPa (1 bar) compiled from the work of Greig and Barth (1938) and Schairer and Bowen (1956) are depicted in Figure 1. Examination of Figure 1 reveals the following liquidus phase relations as the $NaAlSiO_4$ component in the melt increases: a tridymite- and albite-saturated eutectic melt (N_{20}, eutectic I), a thermal divide at the composition albite (N_{33}), an albite- and nepheline$_{ss}$-saturated eutectic melt (N_{41}, eutectic II), and the peritectic composition (N_{60}). Subscripts represent mole percent of $NaAlSiO_4$ in the system $NaAlSiO_4$-SiO_2. Nominal compositions in this system have the common molar ratio Na/Al = 1, and in the molten state at 100 kPa all have fully polymerized network structures. An ideal opportunity is presented to investigate hypotheses that propose relationships between phase equilibria behavior and the structure and dynamics of a system well studied in terms of phase relations (Greig and Barth, 1938; Schairer and Bowen, 1956), spectroscopy (Sharma et al., 1978; Taylor and Brown, 1979a, 1979b; McMillan et al., 1982; Seifert et al., 1982), and thermochemistry (Navrotsky et al., 1982; Richet and Bottinga, 1984) at 100 kPa. Furthermore, the composition $NaAlSi_2O_6$ (N_{50}) occurs in this system. It has been noted that in crystalline $NaAlSi_2O_6$ (jadeite), all Al is [6]Al. In contrast, melt of jadeite composition is dominated by [4]Al, at least at pressures $< \sim 4$ GPa (Sharma et al., 1979; Ohtani et al., 1985; Hamilton et al., 1986).

In order to understand better the connection between melt structure and melt dynamics, we have undertaken an experimental study of viscosity in the system $NaAlSiO_4$-SiO_2 determined by concentric cylinder rheometry. Rheometric data have been collected for seven compositions in this system, over the range of temperatures from 1350 to 1000 °C and with pressure at 100 kPa, at shear rates from 0.01 to 8.7/s for single-phase melts and supercooled liquids with compositions from N_{20} to N_{60}. For many of these compositions, no data previously existed. In this investigation, we compare and combine our data with those of other workers, paying particular attention to the compositional variation of viscosity and its temperature derivative, and speculate on the physical sig-
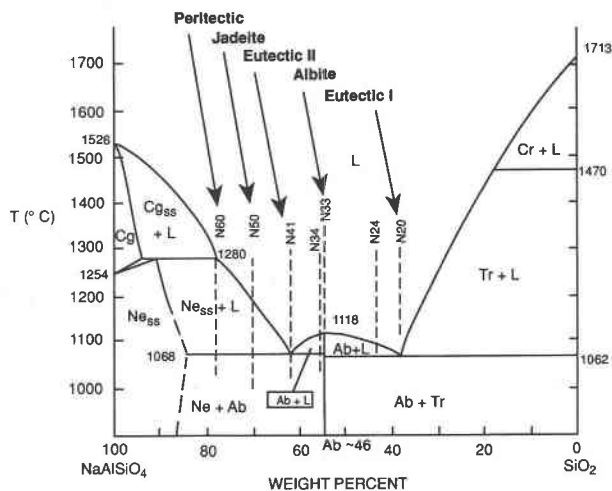

Fig. 1. Phase diagram of the system $NaAlSiO_4$-SiO_2, based on the work of Greig and Barth (1938) and Schairer and Bowen (1956). Composition axis is in weight percent of $NaAlSiO_4$ component; note that in text compositions are referred to in mole percent of $NaAlSiO_4$ component. Temperatures are noted in degrees Celsius, including specified invariant points. Dashed vertical lines represent temperature range sampled for each composition in viscometric experiments; labels refer to sample numbers in Table 1. Abbreviations for the various phases in the system are Ab = albite; Cg = carnegieite; Cg$_{ss}$ = carnegieite-albite solid solution; Ne = nepheline; Ne$_{ss}$ = nepheline solid solution; Cr = cristobalite; L = liquid; Tr = tridymite.

nificance of the observations. In concurrent studies, the technique of molecular dynamics is used to understand the relationships between melt structure and the thermodynamic and transport properties in this system (Stein et al., 1992a, 1992b). On the atomic scale, the molecular dynamics studies rationalize the relationships discovered experimentally (see also Scamehorn and Angell, 1991) and direct attention to further experimental studies needed to elucidate the microscopic to macroscopic connection.

EXPERIMENTAL MEASUREMENTS

Sample preparation

The viscometric data of this study were collected for compositions along the join $NaAlSiO_4$-SiO_2, denoted by the mole fraction of $NaAlSiO_4$ (N_{100}). Nominal compositions include (in mole percent) N_{20} (the albite-tridymite eutectic, hereafter labeled eutectic I), N_{24} (near eutectic I), N_{33} (the albite thermal divide, ab), N_{34} (near albite), N_{41} (the albite-nepheline$_{ss}$ eutectic, hereafter labeled eutectic II), N_{50} (jadeite, jd), and N_{60} (peritectic). Nominal and experimental compositions are collected in Table 1 and are indicated on the 100-kPa phase diagram of Figure 1. Starting glasses were prepared by mixing appropriate proportions of reagent grade Na_2CO_3, Al_2O_3, and silica. Batches were dry-mixed, ground, and decarbonated at 850 °C. Decarbonated products were then fused and

TABLE 1. Nominal and analyzed compositions of viscometric samples

Sample	Viscometric experiment	Na_2O (wt%)	Al_2O_3 (wt%)	SiO_2 (wt%)	Total
N20 (eutectic I)	JS132.3	8.1(8.1)*	13.6(13.3)*	78.1(78.6)*	99.8
N24	JS131.2	10.3(10.6)	17.3(17.5)	71.6(71.9)	99.2
N33A (ab)	JS115	12.6(12.8)	20.7(21.1)	66.0(66.1)	99.3
N33B** (ab)	JS121		Same as JS115		
N34	JS129	12.0(11.8)	20.1(19.4)	67.2(68.7)	99.1
N41 (eutectic II)	JS130	13.8(14.2)*	23.1(23.4)*	61.5(62.4)*	98.4
N50A (jd)	JS118	15.9(15.3)	25.6(25.2)	58.0(59.4)	99.5
N50B (jd)	JS123	15.4	24.3	60.0	99.7
N50C** (jd)	JS128.2		Same as JS123		
N60A (peritectic)	JS117	18.0(17.5)*	27.2(28.8)*	53.1(53.7)*	98.3
N60B (peritectic)	JS127.2	17.6	27.4	53.7	98.7
N60C (peritectic)	JS127UP		Same as JS127.2		

Note: Nominal compositions indicated by parentheses. The compositions corresponding to albite and jadeite are abbreviated as ab and jd, respectively.
 * Nominal composition for ternary invariant points of system $Na_2O-Al_2O_3-SiO_2$ (Schairer and Bowen, 1956).
 ** Replicate measurements.

ground in several cycles to produce homogeneous glass chips. Samples were analyzed at the end of viscometric experiments, and compositions are within acceptable tolerances of nominal values, which have molar Na/Al equal to unity. Quenched glasses were analyzed by electron microprobe using standard techniques with special effort to avoid volatilization of Na. After viscometric measurements, samples were examined for bubbles and any evidence of specimen heterogeneity. Bubble contents were generally <1 vol%; bubbles when present were rather uniformly distributed within the sample. All measurements were made in air at 100 kPa.

Rheometric measurements

The design, construction, and calibration of the high-torque concentric cylinder rheometer used in this study have been previously described (Spera et al., 1988). Periodic standardization using NBS borosilicate glass 717 throughout the period of investigation indicated an accuracy of about 0.05 in log η, slightly poorer than the NBS-quoted uncertainty of 0.03 in log η for NBS 717. Temperatures were accurate to ±3 K. The physical measurement consisted of a precisely determined rotor rotation rate paired with a measured rotor torque. A discussion of the experimental methodology may be found elsewhere (Spera et al., 1988). Table 2 lists the radial dimensions of the rotors (R_r), cylindrical crucibles (R_c), and rotor immersion depths (h) for each experiment. Once a given sample of bubble-free homogeneous glass was loaded into the cup of the rheometer, isothermal measurements were made starting at the high-temperature end of the desired range. At each temperature, torque data were collected throughout the broadest possible range in shear rate, given the limitations of the rheometer and the high viscosity of some of the compositions. At the end of each isothermal experiment, the temperature was raised to allow the free surface to relax viscously; then the temperature was dropped to a new value, and the procedure was repeated after thermal reequilibration. The range of temperature for each composition is indicated by a dashed vertical line in Figure 1. Each data point

(consisting of both a rotation rate and torque at a given temperature for a specified composition) is an average of from three to ten individual measurements, each of a duration of 10–100 s.

Data reduction

Experimental values of rotation rate (Ω) and torque (Γ) were analyzed independently of any assumptions regarding constitutive behavior of the melt or supercooled sodium aluminosilicate liquid. By this method, details of which are contained in Spera et al. (1988), unique values for the shear stress ($\tau_{r\theta}$) and shear rate ($\dot{\gamma}_{r\theta}$) and their respective uncertainties were recovered from the raw experimental data. The power law model was found to be the most general model justified by the data, according to rigorous application of the F statistic to a sequence of power series regressions of log Ω against log $\tau_{r\theta}$. At a given temperature and composition, the power law model gives

$$\tau_{r\theta} = m\dot{\gamma}_{r\theta}^n \qquad (1)$$

in which m and n are determined, respectively, from the intercept and slope of the linear regression of log Ω vs. log $\tau_{r\theta}$ for a set of isothermal rheometric data. That is, once the regression parameters a_0 and a_1 in the expression

$$\log \Omega = a_0 + a_1 \log \tau_{r\theta} \qquad (2)$$

are found, the power law parameters are then computed according to

$$m = \left[\frac{10^{-a_0}(1 - C^{a_1})}{2a_1}\right]^{1/a_1} \qquad (3a)$$

$$n = a_1^{-1} \qquad (3b)$$

with $C = (R_r/R_c)^2$ in Equation 3a. Note that Equation 3a corrects a typographical error in Spera et al. (1988), which also includes a derivation of Equation 3. A practical difficulty encountered in the reduction of isothermal τ-$\dot{\gamma}$ data is that without sufficient range in shear rate, the value of the power law exponent n may be inaccurately determined (Borgia and Spera, 1990; Stein and Spera, 1992). For silicate melts, with estimated power law exponents

Sample	R_c (cm)	R_r (cm)	h (cm)
N20	1.413	0.483	2.502
N24	1.454	0.477	4.572
N33A	1.270	0.500	2.873
N33B	1.270	0.477	3.886
N34	1.508	0.477	4.801
N41	1.457	0.477	4.369
N50A	1.270	0.473	4.128
N50B	1.468	0.477	2.329
N50C	1.468	0.476	4.750
N60A	1.270	0.476	3.352
N60B	1.270	0.476	3.352
N60C	1.270	0.476	3.352

Note: Sample numbers correspond to those given for viscometric experiments in Table 1. R_c is the radius of the cylindrical crucible. R_r is the rotor radius. The symbol h is the depth of immersion of the rotor.

close to unity ($0.8 \leq n \leq 1$), simple forward modeling calculations show that the ratio of maximum to minimum shear rate ought to be at least 50–100 to recover an accurate value of the power law exponent (n) from concentric cylinder rheometric data exhibiting typical experimental uncertainties. Because limitations inherent in the design of the rheometer preclude the measurement of torque for a suitably large variation of rotation rate in the aluminosilicate system, we chose not to incorporate the power law parameters explicitly into the viscosity-temperature relationship. Instead, we adopted a procedure whereby the extracted power law parameters m and n, along with their uncertainties, were used to determine a single viscosity (η) and a measure of its uncertainty (σ_η) at each temperature, allowing for instrumental errors. Viscosities were computed according to the relation

$$\eta = \frac{\tau}{\dot\gamma} = m\dot\gamma^{n-1} \qquad (4)$$

at each temperature from individual pairs of shear stress ($\tau_{r\,\theta}$) and shear rate ($\dot\gamma_{r\,\theta}$). Uncertainty in viscosity was calculated based on propagation of errors in the power law coefficients m and n. We have chosen the power law analysis specifically to avoid a priori assumptions regarding constitutive behavior. In order to test the robustness and validity of the data reduction methodology, we used the raw $\tau_{r\,\theta}$-Ω data, together with the standard (Margules) expression for Newtonian viscosity, as a function of Γ, Ω, and C to compute η and σ_η. The viscosities computed by each method were indistinguishable within the limits of uncertainty. We observed a departure from Newtonian flow (i.e., $n \neq 1$) in the few experiments for which $\dot\gamma_{max}/\dot\gamma_{min} > 50$, e.g., $N24$ at 1200 °C, $N41$ at 1125 °C, N_{50B} at 1200 °C. In all cases the departure remained rather small and the power law parameter n was less than or equal to unity (see Table 3).[1]

Dingwell and Webb (1989) and Webb and Dingwell (1990) asserted that the onset of non-Newtonian behavior in silicate melts occurs due to viscoelastic response when the characteristic time scale of an experimental perturbation ($\dot\gamma^{-1}$ in rheometry) is $< \sim 100$–300 times greater than the time scale of the relaxation response of the melt (defined by η/G_∞, where G_∞ is the unrelaxed shear modulus). From routine analysis of our experimental conditions, it is evident that this limit was never exceeded in our experiments because of the dynamic limitations of the rheometer. Unfortunately, the power law analysis being presented here neither demonstrates nor excludes small departures from Newtonian behavior in the relaxed melt regime. If the above examples are to be accepted, they cannot be explained by the onset of viscoelastic response in these melts.

Results

Table 3 presents for each composition and temperature the number of data points in the regression of log Ω and log $\tau_{r\,\theta}$, the correlation coefficient of the regression defined by Equation 2, the range of experimental shear rate and shear stress, and the derived power law parameters, including their respective uncertainties. Several important features of the data should be noted. Correlation of the raw Ω-$\tau_{r\,\theta}$ data by Equation 2 is generally excellent, with r^2 values >0.96 in most cases. The number of data points used in the fundamental regression varies somewhat but averages around 20–30 individual Ω-$\tau_{r\,\theta}$ pairs for a given composition at a fixed temperature. For some compositions, such as $NaAlSi_2O_6$ melt (e.g., N_{50B}), as many as 75 Ω-$\tau_{r\,\theta}$ pairs were utilized in the regression, and the correlation at high temperature exceeds 0.98. Examination of the shear rate and shear stress range for specific compositions along an isotherm shows a wide variance. On average, measurements span a range in shear rates of about a factor of 10–15, with a maximum range of 80 and minimal values around 2. The 1σ uncertainties in the parameters m and n collected in Table 3 refer to the precision of the measurements and not their inherent accuracy.

Temperature dependence

Viscosity values, including 1σ errors, for each isothermal experiment are given in Table 4. Sample numbers are those used in Table 1. Figure 2a–2g shows the viscosity-inverse temperature data for each composition; when multiple measurements were made on a single composition (e.g., N_{33}, N_{50}, and N_{60}), data are combined on a single plot. Presented on each plot are the computed activation energy for viscous flow from the Arrhenian model ($B = E_\eta/R$)

$$\log \eta = A + \frac{B}{T} \qquad (5)$$

and the range of shear rates in the entire set of rheometric data for that composition. Error bars ($\pm 1\sigma$) for each computed viscosity are shown with each point. To aid comparison, the horizontal axes are identical and the vertical axes employ a uniform scale for each plot. In general, the
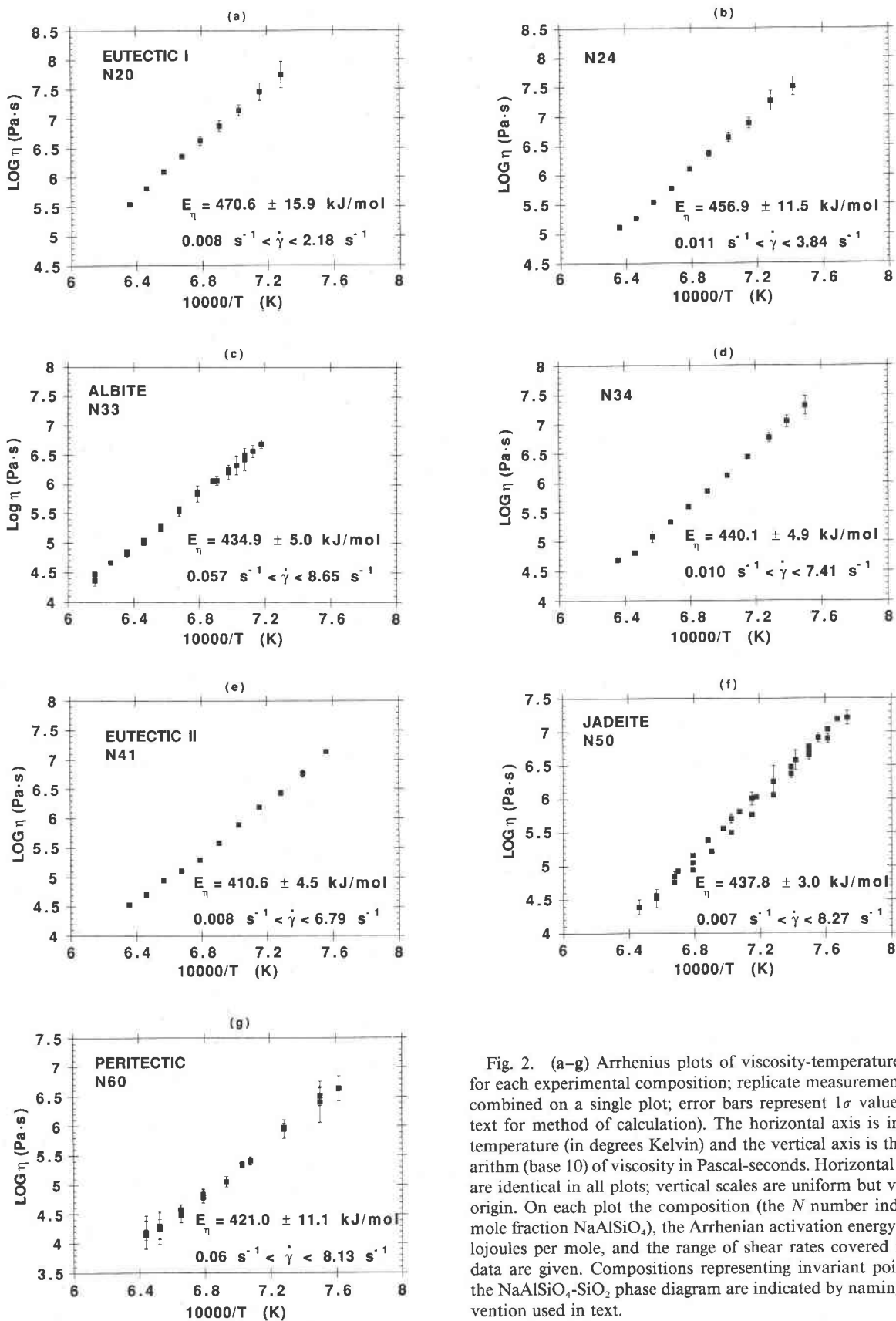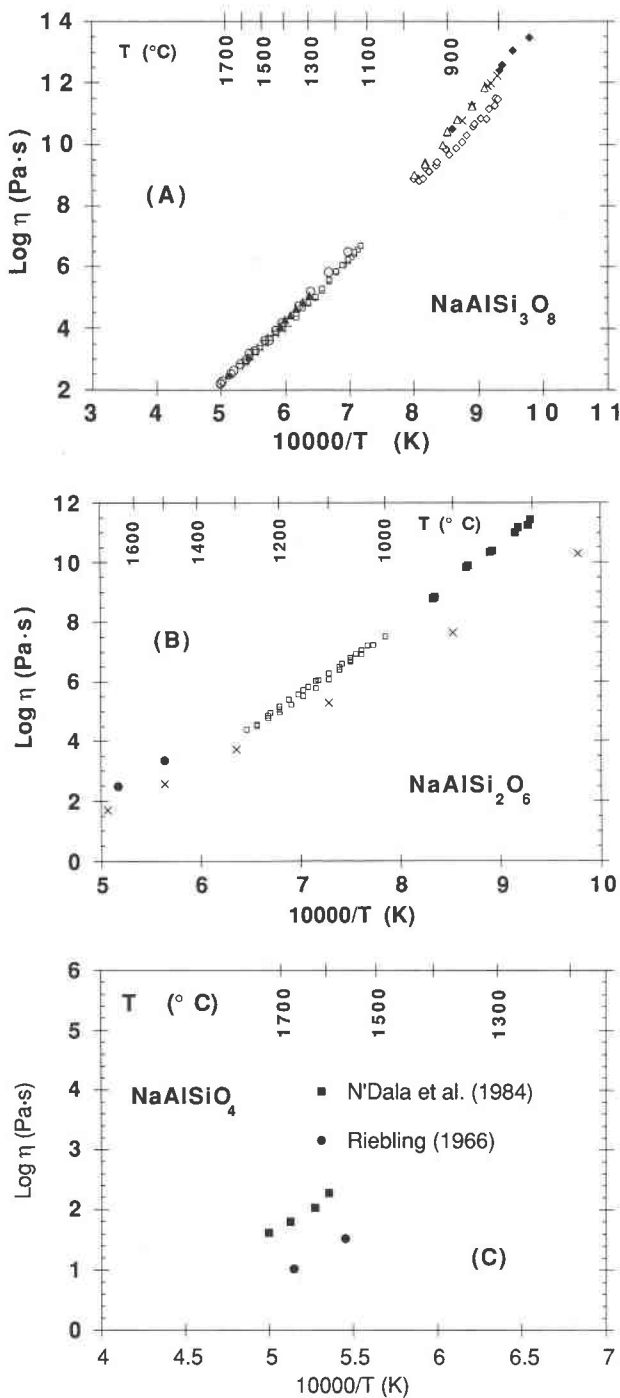
Fig. 2. (a–g) Arrhenius plots of viscosity-temperature data for each experimental composition; replicate measurements are combined on a single plot; error bars represent 1σ values (see text for method of calculation). The horizontal axis is inverse temperature (in degrees Kelvin) and the vertical axis is the logarithm (base 10) of viscosity in Pascal-seconds. Horizontal scales are identical in all plots; vertical scales are uniform but vary in origin. On each plot the composition (the N number indicates mole fraction $NaAlSiO_4$), the Arrhenian activation energy in kilojoules per mole, and the range of shear rates covered in the data are given. Compositions representing invariant points of the $NaAlSiO_4$-SiO_2 phase diagram are indicated by naming convention used in text.

TABLE 4. Summary of viscosity

T (°C)	$\log \eta$ (Pa·s)[*]	$\sigma_{\log \eta}$[**]	T (°C)	$\log \eta$ (Pa·s)[*]	$\sigma_{\log \eta}$[**]
	N20			**N50A**	
1300	5.533	0.039	1275	4.391	0.109
1275	5.804	0.021	1250	4.519	0.136
1250	6.097	0.041	1225	4.842	0.080
1225	6.358	0.027	1200	5.051	0.035
1200	6.630	0.080	1150	5.704	0.065
1175	6.880	0.089	1125	6.003	0.095
1150	7.140	0.092	1100	6.260	0.238
1125	7.452	0.148	1075	6.580	0.145
1100	7.739	0.224	1060	6.702	0.015
	N24			**N50B**	
1300	5.103	0.041	1220	4.928	0.016
1275	5.255	0.022	1200	5.153	0.010
1250	5.525	0.019	1180	5.380	0.011
1225	5.760	0.022	1160	5.557	0.008
1200	6.102	0.027	1140	5.807	0.013
1175	6.369	0.053	1120	6.028	0.013
1150	6.642	0.077	1100	6.257	0.031
1125	6.881	0.090	1080	6.475	0.026
1100	7.254	0.171	1060	6.781	0.026
1075	7.500	0.157	1050	6.915	0.066
			1040	7.035	0.036
			1030	7.189	0.033
	N33A			**N50C**	
1350	4.365	0.094	1250	4.562	0.021
1300	4.816	0.048	1225	4.758	0.022
1275	4.998	0.032	1200	4.947	0.017
1250	5.228	0.035	1175	5.216	0.017
1225	5.532	0.081	1150	5.495	0.018
1200	5.835	0.138	1125	5.762	0.015
1175	6.063	0.081	1100	6.055	0.031
1160	6.202	0.126	1080	6.374	0.061
1150	6.325	0.163	1060	6.656	0.069
1140	6.427	0.194	1040	6.900	0.070
1130	6.566	0.103	1020	7.207	0.104
	N33B			**N60A**	
1350	4.471	0.036	1260	4.302	0.229
1325	4.663	0.018	1230	4.489	0.120
1300	4.848	0.017	1200	4.790	0.095
1275	5.037	0.012	1170	5.052	0.089
1250	5.294	0.012	1140	5.412	0.068
1225	5.580	0.011	1100	5.951	0.158
1200	5.859	0.022	1060	6.409	0.349
1180	6.057	0.029	1040	6.635	0.213
1160	6.254	0.033			
1140	6.500	0.043			
1120	6.689	0.072			
	N34			**N60B**	
1300	4.686	0.023	1260	4.249	0.167
1275	4.806	0.013	1230	4.512	0.151
1250	5.078	0.102	1200	4.830	0.090
1225	5.327	0.014	1150	5.340	0.052
1200	5.593	0.016	1100	5.977	0.070
1175	5.858	0.021	1060	6.505	0.160
1150	6.127	0.019			
1125	6.447	0.024			
1100	6.775	0.074			
1080	7.050	0.100			
1060	7.317	0.163			
	N41			**N60C**	
1300	4.530	0.023	1280	4.151	0.087
1275	4.702	0.026	1260	4.275	0.282
1250	4.945	0.017	1230	4.575	0.038
1225	5.107	0.021	1200	4.836	0.097
1200	5.290	0.031	1150	5.348	0.056
1175	5.573	0.028	1100	5.949	0.036
1150	5.887	0.031	1060	6.518	0.128
1125	6.188	0.036			
1100	6.431	0.045			
1075	6.764	0.059			
1050	7.138	0.030			

[*] The viscosity at each temperature is an average computed by the method presented in the text.
[**] Standard deviation (1σ value) is computed from propagation of errors in the power law parameters m and n, according to the method presented in the text.

(A)

$NaAlSi_3O_8$

(B)

$NaAlSi_2O_6$

$NaAlSiO_4$

■ N'Dala et al. (1984)

● Riebling (1966)

(C)

←

Fig. 3. (A) Plot of viscosity vs. inverse temperature for albite composition. Lower horizontal scale is inverse temperature; corresponding temperatures in degrees Celsius are indicated on upper horizontal scale. Symbols for Riebling (1966) represent end points of Riebling's temperature range; data were reported only as regression parameters and a temperature range, with no information on the actual number of data points nor estimates of their quality. Low-temperature data points from Taylor and Rindone (1970), Dietz et al. (1970), and Cranmer and Uhlmann (1981b) were read from their published graphical presentations. The following symbols are used in the figure: open circles = Urbain et al. (1982); solid circles = Riebling (1966); open squares = present study; solid triangles = Kozu and Kani (1935); + = Scarfe and Cronin (1986); open triangles = Hummel and Arndt (1985); open diamonds = Cranmer and Uhlmann (1981b); solid diamonds = Dietz et al. (1970); × = Taylor and Rindone (1970). (B) Plot of viscosity vs. inverse temperature for jadeite composition. Lower horizontal scale is inverse temperature; corresponding temperatures in degrees Celsius are indicated on upper horizontal scale. Symbols for Riebling (1966) represent end points of Riebling's temperature range; data were reported only as regression parameters and a temperature range; low-temperature data from Taylor and Rindone (1970) were read from their published graphical presentation. Data reported by Hunold and Brückner (1980) differ considerably from the remainder of the data set and are not used in statistical analyses reported elsewhere in this paper. Symbols: open squares = present study; × = Hunold and Brückner (1980); solid circles = Riebling (1966); solid squares = Taylor and Rindone (1970). (C) Plot of viscosity vs. inverse temperature data for nepheline composition. The regression published by Riebling (1966) for nepheline composition is represented by the end points of the range of temperatures reported.

As an exercise, polythermal viscometric data for each of the seven compositions investigated were fitted to the three-parameter Fulcher expression

$$\log \eta = A + \frac{B}{T - T_0} \qquad (6)$$

where A, B, and T_0 are constants for a given melt. Not surprisingly, the quality of each of the log η–T fits was improved using the three-parameter expression as opposed to the two-parameter Arrhenian one. Application of the F statistic shows that the Fulcher fit is statistically significant for three of the compositions (N_{34}, N_{41}, and N_{60}), despite the rather limited temperature range (~250 °C) of the viscometric data. It is also interesting (but perhaps coincidental) that T_0 increases as melts become more $NaAlSiO_4$-rich (e.g., T_0 values for N_{34}, N_{41}, and N_{60} are 550, 780, and 795 K, respectively). This indicates that melts become more non-Arrhenian as the $NaAlSiO_4$ component increases (i.e., more fragile; see Angell, 1988), which is consistent with the more irregular structure of a network in which intertetrahedral distortion accompanies the coupled substitution Na + Al = Si (see below).

The viscosity measurements span a temperature range of nearly 1000 ° when combined with those in the liter-

uncertainties on the individual data points are smallest in the middle of the temperature range, where the range of shear rates examined for a particular temperature is greatest (see Table 3). This condition more precisely determines the power law parameters m and n, from which the errors in viscosity are calculated. The data are well represented by the Arrhenian model in the temperature range studied; correlation coefficients for the η vs. $1/T$ regressions are almost always >0.998.

TABLE 5. Arrhenian parameters

Sample	X_N	A (log Pa·s)	σ_A	B (log Pa·s − K)	σ_B	E_η (kJ/mol)	σ_{E_η}
SiO$_2$	0.000	−7.246	0.078	26932	150	515.6	2.9
N20	0.203	−10.071	0.546	24582	833	470.6	15.9
N24	0.242	−10.144	0.398	23868	600	456.9	11.5
ABBest	0.333	−9.123	0.013	22273	18	426.4	0.3
N33	0.333	−9.603	0.171	22716	261	434.9	5.0
N33U[A]	0.333	−8.606	0.118	21589	205	413.3	3.9
N33K[B]	0.333	−8.686	0.802	21595	523	413.5	10.0
N33S[C]	0.333	−7.197	0.180	18871	318	361.3	6.1
N33TR[D]	0.333	−12.249	0.995	26317	1099	503.9	21.0
N33CU[E]	0.333	−7.930	0.437	20714	504	396.6	9.7
N33H[F]	0.333	−11.962	0.400	26103	468	499.7	9.0
N33D[G]	0.333	−11.522	0.522	25619	559	490.5	10.7
N33R[H]	0.333	−7.086	1.000	18640	1864	356.9	35.7
N34	0.341	−10.016	0.174	22989	258	440.1	4.9
N41	0.408	−9.166	0.160	21449	236	410.6	4.5
JDBest	0.500	−11.735	0.035	24743	48	473.7	0.9
N50	0.500	−10.433	0.109	22870	156	437.8	3.0
N50TR[D]	0.500	−13.186	0.656	26435	739	506.1	14.2
N50R[H]	0.500	−7.828	1.000	18025	1802	345.1	34.5
N60	0.598	−10.085	0.406	21994	581	421.0	11.1
N67R[H]	0.667	−7.486	1.000	17640	1764	337.7	33.8
N79R[H]	0.792	−7.417	1.000	17040	1704	326.3	32.6
NaAlSiO$_4$[H]	1.000	−7.320	1.000	16220	1622	310.5	31.1
NaAlSiO$_4$[I]	1.000	−7.314	1.011	17825	1950	341.2	37.3

Note: Sample numbers from this study are those given in Table 1. X_N is the mole fraction of NaAlSiO$_4$ component, A and B are the coefficients of the Arrhenian model of Eq. 5 (uncertainties σ). Activation energy for viscous flow (in kilojoules per mole) and its uncertainty are calculated directly from values of B. ABBest and JDBest are parameters for albite and jadeite, respectively, from combined data sets as described in text.
Results from previously published studies: A = Urbain et al. (1982); B = Kozu and Kani (1935); C = Scarfe and Cronin (1986); D = Taylor and Rindone (1970); E = Cranmer and Uhlman (1981b); F = Hummel and Arndt (1985); G = Dietz et al. (1970); H = Riebling (1966); I = N'Dala et al. (1984).

ature from Kozu and Kani (1935), Riebling (1966), Dietz et al. (1970), Taylor and Rindone (1970), Hunold and Brückner (1980), Cranmer and Uhlmann (1981b), Urbain et al. (1982), N'Dala et al. (1984), and Hummel and Arndt (1985) for the compositions NaAlSi$_3$O$_8$ (albite, N_{33}) and NaAlSi$_2$O$_6$ (jadeite, N_{50}). Figure 3A shows the results for NaAlSi$_3$O$_8$ combined with literature values and Figure 3B shows results for NaAlSi$_2$O$_6$. Figure 3C shows the limited data available for nepheline composition (NaAlSiO$_4$). Figure 3A–3C portrays all relevant data known to us for these compositions.

The data for albite composition melt at superliquidus temperatures in the range 1120–1700 °C show remarkable consistency among five investigators (Fig. 3A). Arrhenian parameters for all individual investigators are given in Table 5. Arrhenian parameters for a best fit of all available results for molten and supercooled albite in the temperature range 800–1720 °C are also listed in the table, in the entry labeled ABBest. Proper treatment of the errors, either as originally reported or estimated by us, that accounts for the methods used and their general accuracies has been included in the derivation of the Arrhenian parameters collected in Table 5. The data of Riebling (1966) for NaAlSi$_3$O$_8$ melt yield a considerably smaller activation energy and larger intercept and are restricted to a small range of relatively high temperatures. Unfortunately it is impossible to rate the quality of Riebling's viscometric data. Raw experimental data are not reported by Riebling; only regression (Arrhenian) parameters are given, and no uncertainties are reported for the regression constants. In light of these omissions, we have

chosen not to include Riebling's data in fitting the overall data set to the Arrhenian model (ABBest), based on combining our data (open squares on Fig. 3A) with those of previous workers.

The data for jadeite composition from the present work, combined with those of Taylor and Rindone (1970), cover a temperature range from 800 to nearly 1300 °C (Fig. 3B). The entire data set shows less consistency than that for albite: the results of Hunold and Brückner (1980) vary considerably from the remainder of the data, and we therefore disregard their results. It is interesting to note that Richet (1984) rejected the results of Hunold and Brückner (1980) as being inconsistent with the high-temperature viscometric data of Riebling (1966) and the low-temperature viscometric data of Taylor and Rindone (1970) on jadeite composition melt. Our new results on jadeite composition (N_{50A}, N_{50B}, N_{50C}) support Richet's argument. The viscometric data of Hunold and Brückner on jadeite melt appear to be too low (about 0.5–1.0 in log η) in the temperature range of our experiments (1293–1548 K; see Fig. 3B). At low temperatures (i.e., around the glass transition temperature T_g) the discrepancy between the results of Taylor and Rindone (1970) and Hunold and Brückner (1980) is greater than an order of magnitude. Riebling (1966) gives a significantly smaller activation energy for NaAlSi$_2$O$_6$ melt compared with our values, and, for the reasons presented above, we also chose to exclude Riebling's data in fitting the Arrhenius relation for jadeite melt (labeled JDBest in Table 5), using only our data and those of Taylor and Rindone at low temperatures.

TABLE 6. Statistical tests of Arrhenian vs. Fulcher equations

Sample	Eq. in text	N^*	Coefficients	Error est.	χ^2	F_{reg}^{**} $F_{add}†$
Albite	5	95	$A = -9.123$ $B = 22273$	0.013 18	10126	10363
Albite	6	95	$A = -5.994$ $B = 14219$ $T_0 = 273.9$	0.058 131 4.9	8105	6716 (17.9) $F_{crit}‡ = 11.9$
Jadeite	5	42	$A = -11.735$ $B = 24743$	0.035 48	909.4	13906
Jadeite	6	42	$A = -7.294$ $B = 14560$ $T_0 = 297.1$	0.245 480 15.7	697.5	11800 (20.8) $F_{crit}‡ = 12.6$

Uncertainties in log η for data sources used in regressions

Urbain et al. (1982)	0.02
Dietz et al. (1970)	0.05
Scarfe and Cronin (1986)	0.05
Kozu and Kani (1935)	0.05
Taylor and Rindone (1970)	0.02
Cranmer and Uhlmann (1981b)	0.02
Hummel and Arndt (1985)	0.05

* N is the number of data points in each regression.
** F_{reg} is the F test of the overall regression.
† F_{add} is the result of the F test for the significance of the added term in the three-parameter model.
‡ F_{crit} is the minimum value of F_{add} required to denote significance for the additional term at the 0.999 level.

Data for nepheline composition are quite limited. Figure 3C shows that the two sets of available measurements differ consistently by nearly a full log unit in viscosity and that the activation energy published by Riebling, as with his data for $NaAlSi_3O_8$ and $NaAlSi_2O_6$ melt, is significantly lower than that computed from the data of N'Dala et al. (1984). It is clear that additional high- and low-temperature measurements on $NaAlSiO_4$ and $NaAlSi_2O_6$ melts and additional low-temperature measurements on $NaAlSi_3O_8$ would be beneficial to evaluate the degree of departure from Arrhenian behavior.

The Arrhenius relation is a semiempirical correlation, known to be inadequate to model data for viscosity vs. temperature data over a wide temperature range for many substances. For most of the compositions examined in the present study, the temperature range of the viscosity data was 200 °C or less, barely adequate to resolve departures from Arrhenian behavior. For albite and jadeite compositions, however, the range of temperatures is >800 °C. This allowed for a more definitive testing of the three-parameter Fulcher model of temperature variation (Eq. 6). Recent applications of free volume theory (Cohen and Turnbull, 1959) and the Fulcher equation in studies of viscosity of silicate melts and supercooled liquids include the work of Cranmer and Uhlmann (1981a) on the system albite-anorthite, Cranmer and Uhlmann (1981b) on albite, and a review of the literature of oxide and simple silicate viscosities by Richet (1984). Richet (1984) applied the Fulcher equation to available data on albite and jadeite compositions and published values for the three coefficients, using data from Riebling (1966) and Taylor and Rindone (1970) for both albite and jadeite, as well as the data of Urbain et al. (1982) for albite.

Our fits to the Fulcher equation were accomplished by standard nonlinear regression using the Levenberg-Marquardt technique (Press et al., 1986) and include results from this study, which was not available to Richet (1984). We combined our results with those of Kozu and Kani (1935), Taylor and Rindone (1970), Dietz et al. (1970), Cranmer and Uhlmann (1981b), Urbain et al. (1982), Hummel and Arndt (1985), and Scarfe and Cronin (1986) for molten $NaAlSi_3O_8$ and with those of Taylor and Rindone (1970) for molten $NaAlSi_2O_6$, excluding in both cases the results of Riebling (1966) for reasons cited earlier. We included low-temperature data from Cranmer and Uhlmann (1981b), which Richet (1984) chose to exclude as seeming less precise. Results of the nonlinear fitting are presented in Table 6, which lists the sample number and composition, along with the equation number (either Eq. 5 or Eq. 6 in the text) to which the parameters correspond, the values of the fit parameters and their uncertainties, the χ^2 value of the regression, and the results of the F test for each regression. Both two- and three-parameter regressions fit the data very well. Notably, our results indicate that for both $NaAlSi_3O_8$ and $NaAlSi_2O_6$ melts, the Fulcher model is statistically significant, given appropriate estimates of experimental uncertainties and proper weighting of individual measurements.

There are indications from the above results on N_{33} and N_{50} and from the results presented earlier on N_{34}, N_{41}, and N_{60} that melts and supercooled liquids in this system are described increasingly better by the Fulcher equation as composition changes from SiO_2 toward $NaAlSiO_4$. In Table 5, the low-temperature data of Taylor and Rindone (1970) give the highest activation energies, whereas the high-temperature measurements of Riebling (1966) systematically yield the lowest ones, and the spread is greater for jadeite than for albite. As Richet (1984) found, T_0 for albite is less than that for jadeite, although we find it only marginally so; the magnitude of T_0 is one measure of the degree of departure from Arrhenian behavior. Clearly, as $T_0 \to 0$, the three-parameter Fulcher model collapses into the two-parameter Arrhenian one.

Richet's T_0 values and those found in the present study are quite similar for $NaAlSi_3O_8$ (Richet obtained 277 K, whereas we find 274 ± 5 K) but rather different for $NaAlSi_2O_6$. Richet obtained 477 K for $NaAlSi_2O_6$, but our value is only 297 ± 16 K, similar to the value for $NaAlSi_3O_8$. The difference may be explained by our inclusion of new results on $NaAlSi_2O_6$ and by Richet's inclusion of Riebling's results, which we have disregarded. The new result indicates significantly less non-Arrhenian behavior for $NaAlSi_2O_6$ than was found by Richet. Figure 4 shows the logarithmic viscosity results for $NaAlSi_3O_8$ and $NaAlSi_2O_6$ plotted against T_g/T, using values of T_g published by Richet and Bottinga (1984). The greater curvature of the data for $NaAlSi_2O_6$ when compared with that for $NaAlSi_3O_8$ is visible evidence of the increased non-Arrhenian character (i.e., greater fragility) of $NaAlSi_2O_6$ melt compared with $NaAlSi_3O_8$ melt. Further high quality viscosity measurements, particularly at tempera-
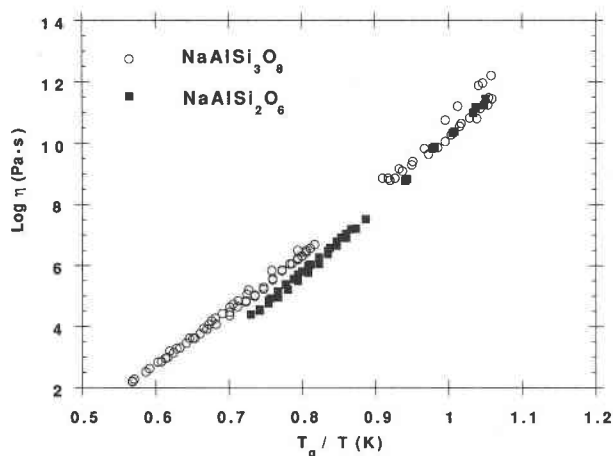
Fig. 4. Plot of log viscosity (Pascal-seconds) vs. T_g/T for albite- and jadeite-composition data (includes all data except Riebling, 1966, and Hunold and Brückner, 1980; T_g is calorimetric glass transition temperature reported by Richet and Bottinga, 1984). A plot in these coordinates allows comparison of degree of curvature in each data set; a larger T_0 (i.e., greater curvature) indicates greater departure from the Arrhenian temperature variation for $NaAlSi_2O_6$ melt.

Fig. 5. Plot of viscosity (Pascal-seconds) vs. composition in terms of mole fraction $NaAlSiO_4$ along the 1673 K isotherm, including results from previous studies listed in Table 5. Some points are extrapolations using Arrhenian parameters from Table 5.

tures approaching T_g, and careful evaluation of experimental uncertainties, will be needed in order to resolve this issue and establish unequivocally whether T_0 does increase with increasing mole fraction of $NaAlSiO_4$ as speculated here.

Composition dependence

Figure 5 is a portrayal of results in the form of an isotherm plot of log viscosity vs. composition in terms of the mole fraction of $NaAlSiO_4$ at 1673 K. There is a systematic decrease of viscosity with increasing $NaAlSiO_4$ content. Most of the decrease occurs between pure silica and eutectic I, although it is clear that for $X_{NaAlSiO_4}$ (hereafter X_N) ≥ 0.2, there is a log-linear relationship between viscosity and composition. Along the 1673-K isotherm for example, there is a decrease by a factor of 50 in the viscosity from eutectic I melt ($X_N = 0.2$) at 32000 Pa·s to pure $NaAlSiO_4$ melt at 2190 Pa·s. There may also be a log-linear relationship between viscosity and composition between pure silica (5×10^8 Pa·s) and eutectic I melt ($X_N = 0.2$, $\eta = 32000$ Pa·s), although there are not enough data in this compositional range to determine precisely the form of the dependence. The structural interpretation of the drastic reduction of viscosity by the addition of metal oxides (e.g., Na_2O, K_2O, etc.) to silica-rich liquids is generally given in terms of the network-modifying model as originally put forward by Zachariasen (1932). The extent of network modification depends on the number of nonbridging O atoms (NBO), which, of course, is directly related to the concentration of the metal oxide additive. The data presented in Figure 5 cannot be rationalized in such a simple fashion. It is obvious from the stoichiometry of the coupled substitution Na^+
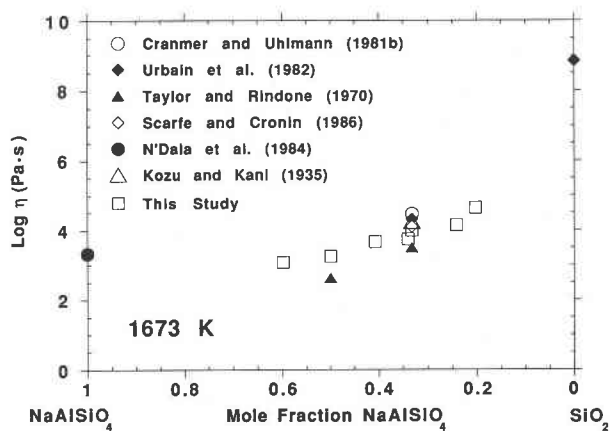
$+ {}^{[4]}Al^{3+} = {}^{[4]}Si^{4+}$ that the addition of $NaAlSiO_4$ does not break down the network structure per se. Since Al is primarily in fourfold coordination and Na serves to balance the charge, $NaAlSiO_4$-rich melt is a network fluid with O coordination numbers near 2 and tetrahedral cation (Al or Si) coordination numbers around 4, as in pure SiO_2 melt at 100 kPa (e.g., Rustad et al., 1991a, 1991b, 1992). Thus the negative value of $(\partial \log \eta/\partial X_N)_{P,T}$, as determined experimentally for melts in the system $NaAlSiO_4$-SiO_2, is not caused by a significant increase in the concentration of NBO. We speculate that topological and bond energy considerations must be important factors. Na-O and Al-O bond lengths are greater than Si-O lengths; similarly, the Si-O bond energy is ~20% greater than the Al-O energy. Substitution of (Na,Al) for Si must induce some random irregularity of the T-O Voronoi polyhedra beyond that usually ascribed to the amorphous state and must broaden the distribution of intertetrahedral TOT angles, as well as displace the mean angle to lower values. Currently, we are pursuing MD simulations (Stein et al., 1992a, 1992b) to gain further insight into the characteristics of induced network distortion as $NaAlO_2$ is added to molten SiO_2 (see also Scamehorn and Angell, 1991).

The variation of viscous activation energy with composition is shown in Figure 6, in which a trend of decreasing activation energy with increasing $NaAlSiO_4$ content is evident. This figure includes results from our experiments, from Urbain et al. (1982) for silica, and from N'Dala et al. (1984) for nepheline melt. The silica value is especially well determined and comes from the exhaustive analysis of Urbain et al. (1982). The value for molten $NaAlSiO_4$ comes from N'Dala et al. (1984), which is slightly higher than the ill-constrained value given by Riebling (1966) (not plotted). For the purpose of maximizing internal consistency, all other values of E_η (i.e., for N_{20}, N_{24}, N_{33}, N_{34}, N_{41}, N_{50}, and N_{60}) were derived exclusively from the present study. The trend of decreas-
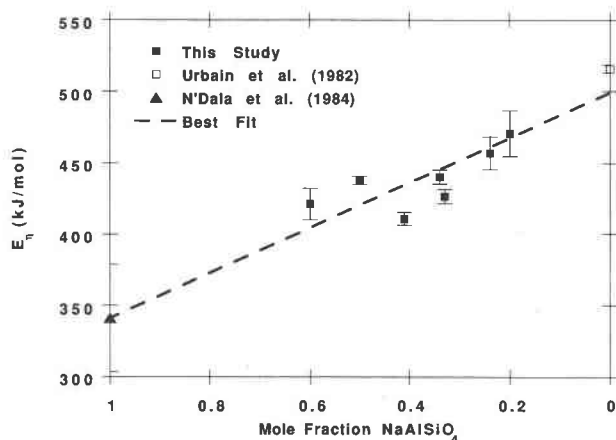
Fig. 6. Activation energy for viscous flow (Arrhenian model, in kilojoules per mole) vs. composition in terms of mole fraction NaAlSiO$_4$ using results from Table 5. Error bars on data points represent uncertainties in E_η (1σ values). Best-fit linear regression line includes data from the present study for intermediate compositions, data of N'Dala et al. (1984) for NaAlSiO$_4$, and data of Urbain et al. (1982) for SiO$_2$.

Fig. 7. Plot of A vs. B from the Arrhenian parameters of Table 5. Perfect compensation would exhibit a linear relationship between the plotted values of A and B. Note that A is proportional to a fictive (logarithmic) viscosity at infinite temperature and that B is proportional to the activation energy for viscous flow (i.e., it is related to the temperature derivative of the viscosity).

ing E_η in Figure 6 is approximately linear for values measured in the range of magmatic temperatures, decreasing from 515 kJ/mol at SiO$_2$ to 340 kJ/mol at NaAlSiO$_4$. Linear regression analysis of the data returned the equation $E_\eta = 499 - 158X_N$, where the activation energy is measured in kilojoules per mole and X_N is the mole fraction of the NaAlSiO$_4$ component in the melt. The correlation coefficient is $r^2 = 0.89$, which indicates that nearly 90% of the variation of E_η can be explained in terms of a linear dependence on mole fraction NaAlSiO$_4$. It is interesting to note that the fractional change in E_η going from SiO$_2$ to NaAlSiO$_4$ melt ($\sim$30%) is about equal to the difference in Si-O and Al-O bond energies. Activation energies for the viscometric data of Taylor and Rindone (1970), measured for NaAlSi$_3$O$_8$ and NaAlSi$_2$O$_6$ at temperatures around T_g appear anomalously high and are not plotted. A similar viscometric technique was used in the same temperature range by Cranmer and Uhlmann (1981b) for NaAlSi$_3$O$_8$, and their value for E_η falls near the range of our values.

Compensation

An additional feature of the rheometric data for this system is seen in Figure 7, in which the Arrhenian parameters A and B are plotted against one another in the form of a compensation plot analogous to those made for diffusion data in silicates. There appears to be a rough correlation, although the problems cited earlier regarding some of the previous studies are apparent. Again, if the data of Riebling (1966) and of Taylor and Rindone (1970) are neglected, a reasonably linear compensation array results (except for silica). Although we have reasons to doubt the quality of some of Riebling's data, no such reasons are immediately apparent for the Arrhenian parameters of Taylor and Rindone.
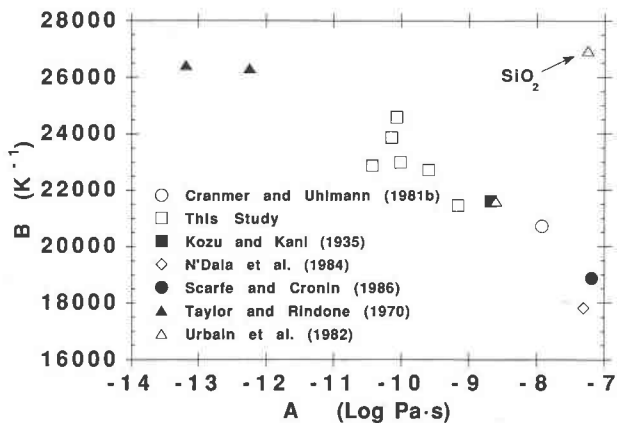
DISCUSSION

The systematic decrease in both the isothermal viscosity and activation energy for viscous flow as NaAlSiO$_4$ is added to molten silica, as depicted in Figures 5 and 6, may be semiquantitatively explained by simple topological and bonding arguments. Indeed there is a large body of evidence upon which to base an explanation, including Raman spectra (Sharma et al., 1978; Mysen et al., 1980; McMillan et al., 1982; Seifert et al., 1982; Matson and Sharma, 1985), X-ray radial distribution studies (Taylor and Brown, 1979a, 1979b; Taylor et al., 1980), molecular orbital calculations (DeJong and Brown, 1980a, 1980b; Gibbs et al., 1981), simulations of molecular dynamics (Scamehorn and Angell, 1991; Stein et al., 1992a, 1992b), noble gas solubilities (Roselieb et al., 1992), and calorimetric studies (Navrotsky et al., 1982).

Substitution of NaAlO$_2$ for SiO$_2$ appears to expand the network structure and introduce distortions in the TO$_4$ network. For example, the volume of a gram-atom of NaAlSi$_3$O$_8$, NaAlSi$_2$O$_6$, and NaAlSiO$_4$ glass at 25 °C is 1.376, 1.386, and 1.422 J/bar per O atom, respectively. In summarizing data for crystalline phases in the system NaAlSiO$_4$-SiO$_2$, Taylor and Brown (1979b) noted that mean TO bond distances increase from 1.59 Å for crystalline SiO$_2$ to 1.67 Å for nepheline. There is also a decrease in the mean intertetrahedral TOT bond angles from 150 to 143° as the T site becomes half-occupied by Al. The decrease in bridging intertetrahedral TOT angles is similar to the observed pressure-induced shift in the Si-O-Si bond-angle distribution maximum from 143 to 138° determined by magic-angle spinning nuclear magnetic resonance experiments on amorphous silica. Devine et al. (1987) have explained the decrease of bridging angle in terms of a reduction in the distance separating O and the second nearest neighbor O from 3.12 to 2.9 Å. Such

a steric effect may also be important in $NaAlSiO_4$-SiO_2 melts as X_N increases isobarically. In ultrasonic studies, Rivers and Carmichael (1987) found that longitudinal sound velocity decreased with composition from molten $NaAlSiO_4$ to molten $NaAlSi_3O_8$. Compressibility (e.g., governed by O-O repulsions) is inversely related to the sound velocity, so the pattern of ultrasonic velocities can be rationalized in terms of inferred changes in intertetrahedral angles. Potential energy curves vs. TOT intertetrahedral bridging angle for $H_6Si_2O_7$ and $H_6SiAlO_7^{-1}$ clusters in molecular orbital calculations by Meagher et al. (1980) gave minimum-energy Si-O and Al-O bond lengths of 1.59 and 1.70 Å, respectively, and minimum-energy bridging angles of 142 and 131° for Si-O-Si and Al-O-Si, in agreement with X-ray data (Taylor et al., 1980). Calorimetrically determined mixing enthalpies in the system $NaAlO_2$-SiO_2 (Navrotsky et al., 1982) show that maximum stabilization occurs at the nepheline composition (1:1 ratio of $NaAlO_2/SiO_2$). The molecular orbital calculations of DeJong and Brown (1980a, 1980b) for aluminosilicate clusters indicate that the exchange reaction ½(Si-O-Si) + ½(Al-O-Al) = Al-O-Si is strongly exothermic, with an approximate enthalpy $\Delta H \sim -210$ kJ/mol. Interestingly, this energetic stabilization is about equal to the experimentally observed decrease in activation energy for viscous flow from SiO_2 (515 kJ/mol) to $NaAlSiO_4$ (350 kJ/mol). Polarization of bridging O atoms in the Al-O-Si network, which is caused by a greater bond length and a larger electronegativity difference between metal and O for Al-O compared with Si-O, makes for a less covalently bonded structure. The greater ionicity of the Al-O bond compared with Si-O, coupled with the increasing occupancy of holes defined by six-membered tetrahedral rings of Na atoms, leads to a smaller average TOT intratetrahedral angle (Okuno and Marumo, 1982), a larger variance in the distribution of TOT angles, and hence smaller TO bond energies. These topological and energetic factors give rise to a weaker network that correlates with a small, but measurable, increase in the degree of non-Arrhenian thermal behavior as $NaAlSiO_4$ concentration increases (i.e., from $NaAlSi_3O_8$ to $NaAlSi_2O_6$ melt), as monitored by the increase in T_0 in the Fulcher equation. The approximate linear relation between E_η and composition is consistent with the gradual weakening of the network. In recent simulations using molecular dynamics on aluminosilicate melts and glasses, Scamehorn and Angell (1991) showed that non-Arrhenian behavior (termed melt fragility) can be correlated with increasing TO length and decreasing TOT angle. If melt fragility does increase with increasing substitution of Na + Al = Si, then one expects an increase of $\Delta C_P/C_P$ at the glass transition temperature as the $NaAlO_2$ content of the glass increases. One also would expect the solubility of noble gases to decrease at constant temperature and pressure upon addition of $NaAlO_2$ to SiO_2 melt because of the greater framework distortion associated with smaller TOT bridging angles and less hole volume availability for a noble gas atom due to increasing occupation of six-

membered ring holes by Na. On the basis of available (but limited) data, these trends are indeed observed (Richet, 1984; Richet and Bottinga, 1984; Roselieb et al., 1992).

In summary, viscometric data in the system $NaAlSiO_4$-SiO_2 can be rationalized in terms of the reduction of the strength of the network associated with introduction of Al into tetrahedral sites, and Na + Al = Si has the effect of producing a weaker network structure, with an activation energy for viscous flow considerably smaller than that for molten silica.

CONCLUSIONS

We have performed measurements of viscosity on melts and supercooled liquids in the system $NaAlSiO_4$-SiO_2, at temperatures from 1000 to 1300 °C at shear rates ranging from 0.01 to 8.7/s using concentric cylinder rheometry. Departure from Newtonian flow is difficult to detect at the conditions of temperature and shear rate of the experiments. However, when measurements are performed over a sufficiently large range of shear rates, it is not possible to exclude non-Newtonian constitutive behavior (with a power law exponent $n < 1$). Systematic compositional variation of viscosity and its temperature derivative are evident from our measurements; these results include data on five compositions spanning the range from 20 to 60 mol% $NaAlSiO_4$, for which no previous data were available. Fitting of the viscosity-temperature data (including estimated uncertainties) to both the Arrhenian and Fulcher models was performed. Statistically significant fits to the three-parameter Fulcher equation result from combination of our data with previously published literature values for the compositions $NaAlSi_3O_8$ and $NaAlSi_2O_6$. These tests give indications that melts in this system exhibit increasingly non-Arrhenian behavior with increasing concentration of $NaAlSiO_4$ component. Results for $NaAlSi_2O_6$ melt in the temperature range 1275–1000 °C confirm that the results of Hunold and Brückner (1980) differ considerably from the remainder of the data, are systematically low by 0.5 to >1 log unit, and should be considered suspect. Properties of melts and glasses in this binary system have been well studied by a variety of techniques, including X-ray diffraction, infrared and Raman spectroscopy, thermochemistry, and computer calculations using molecular dynamics and quantum-chemical (molecular orbital) methods. Results from these studies strongly suggest that introduction of Na and Al with 1:1 molar ratio into molten SiO_2 produces irregular TO_4 intertetrahedral network distortion, in addition to a net reduction of intratetrahedral bond strength due to both the greater Al-O bond length and the polarizing effects of six-membered ring hole filling by Na. These microscopic features give rise to the decrease both in viscosity and in its temperature derivative as $NaAlSiO_4$ is added to silica liquid. Finally, the increasing Vogel temperature (T_0 in the Fulcher expression, Eq. 6), increases upon addition of $NaAlSiO_4$ component to silica melts, a sign of increasing melt fragility.

Acknowledgments

References cited

Angell, C.A. (1988) Perspective on the glass transition. Journal of Physics and Chemistry of Solids, 49, 863–871.

Babcock, C.L. (1968) Substructures in silicate glasses. Journal of the American Ceramic Society, 51, 163–169.

Borgia, A., and Spera, F.J. (1990) Error analysis for reducing noisy wide-gap concentric cylinder rheometric data for nonlinear fluids: Theory and applications. Journal of Rheology, 34, 117–136.

Bottinga, Y., and Weill, D.F. (1972) The viscosity of magmatic silicate liquids: A model for calculation. American Journal of Science, 272, 438–475.

Cohen, M.H., and Turnbull, D. (1959) Molecular transport in liquids and glasses. The Journal of Chemical Physics, 31, 1164–1169.

Cranmer, D., and Uhlmann, D.R. (1981a) Viscosities in the system albite-anorthite. Journal of Geophysical Research, 86, 7951–7956.

———(1981b) Viscosity of liquid albite, a network material. Journal of Non-Crystalline Solids, 45, 283–288.

DeJong, B.H.W.S., and Brown, G.E., Jr. (1980a) Polymerization of silicate and aluminate tetrahedra in glasses, melts, and aqueous solutions. I. Electronic structure of $H_6Si_2O_7$, $H_6AlSiO_7^{1-}$, and $H_6Al_2O_7^{2-}$. Geochimica et Cosmochimica Acta, 44, 491–511.

———(1980b) Polymerization of silicate and aluminate tetrahedra in glasses, melts, and aqueous solutions. II. The network modifying effects of Mg^{2+}, K^+, Na^+, Li^+, H^+, OH^-, F^-, Cl^-, H_2O, CO_2 and H_3O^+ on silicate polymers. Geochimica et Cosmochimica Acta, 44, 1627–1642.

Devine, R.A.B., Dupree, R., Farnan, I., and Capponi, J.J. (1987) Pressure-induced bond-angle variation in amorphous SiO_2. Physical Review B, 35, 2560–2562.

Dietz, E.D., Baak, T., and Blau, H.H. (1970) The superheating of an albite feldspar. Zeitschrift für Kristallographie, 132, 340–360.

Dingwell, D.B., and Virgo, D. (1987) The effect of oxidation state on the viscosity of melts in the system Na_2O-FeO-Fe_2O_3-SiO_2. Geochimica et Cosmochimica Acta, 51, 195–205.

Dingwell, D.B., and Webb, S.L. (1989) Structural relaxation in silicate melts and non-Newtonian rheology in geologic processes. Physics and Chemistry of Minerals, 16, 508–516.

Evans, D.J., and Morriss, G.P. (1990) Statistical mechanics of nonequilibrium liquids, 302 p. Academic, London.

Ferry, J.D. (1980) Viscoelastic properties of polymers, 640 p. Wiley, New York.

Gibbs, G.V., Meagher, E.P., Newton, M.D., and Swanson, D.K. (1981) A comparison of experimental and theoretical bond length and angle variations for minerals, inorganic solids, and molecules. In M. O'Keeffe and A. Navrotsky, Eds., Structure and bonding in crystals, volume I, p. 195–225. Academic, New York.

Greig, J.W., and Barth, T.F.W. (1938) The system Na_2O-Al_2O_3-$2SiO_2$ (nephelite, carnegieite)–Na_2O-Al_2O_3-$6SiO_2$ (albite). American Journal of Science (5th Series), 35A, 93–112.

Hamilton, D.L., Chesworth, W., Kennedy, G., and Fyfe, C. (1986) The absence of 6-fold coordinated Al in jadeite melt near the jadeite liquidus. Geochimica et Cosmochimica Acta, 50, 123–124.

Hansen, J.P., and McDonald, I.R. (1986) Theory of simple liquids (2nd edition), 556 p. Academic, London.

Hummel, W., and Arndt, J. (1985) Variation of viscosity with temperature and composition in the plagioclase system. Contributions to Mineralogy and Petrology, 90, 83–92.

Hunold, K., and Brückner, R. (1980) Physikalische Eigenschaften und struktureller Feinbau von Natrium-Alumosilicatgläsern und -schmelzen. Glastechnische Berichte, 53, 149–161.

Kozu, S., and Kani, K. (1935) Viscosity measurements of the ternary system diopside-albite-anorthite at high temperature. Proceedings of the Imperial Academy of Japan (Tokyo), 11, 383–385.

Kushiro, I. (1976) Changes in viscosity and structure of melt of $NaAlSi_2O_6$ composition at high pressures. Journal of Geophysical Research, 81, 6347–6350.

———(1978) Viscosity and structural changes of albite ($NaAlSi_3O_8$) melt at high pressures. Earth and Planetary Science Letters, 41, 87–90.

Matson, D.W., and Sharma, S.K. (1985) Structures of sodium alumino- and gallosilicate glasses and their germanium analogs. Geochimica et Cosmochimica Acta, 49, 1913–1924.

McMillan, P., Piriou, B., and Navrotsky, A. (1982) A Raman spectroscopic study of glasses along the joins silica-calcium aluminate, silica-sodium aluminate, and silica-potassium aluminate. Geochimica et Cosmochimica Acta, 46, 2021–2037.

Meagher, E.P., Swanson, D.K., and Gibbs, G.V. (1980) The calculation of tetrahedral Si-O and Al-O bridging bond lengths and angles (abs.). Eos, 61 (Supplement), 408.

Mysen, B.O. (1987) Magmatic silicate melts: Relations between bulk composition, structure and properties. In B.O. Mysen, Ed., Magmatic processes: Physicochemical principles, p. 375–399. The Geochemical Society, University Park, Pennsylvania.

———(1988) Structure and properties of silicate melts, 354 p. Elsevier, Amsterdam.

Mysen, B.O., Virgo, D., and Scarfe, C.M. (1980) Relations between the anionic structure and viscosity of silicate melts: A Raman spectroscopic study. American Mineralogist, 65, 690–710.

Navrotsky, A., Peraudeau, G., McMillan, P., and Coutures, J.-P. (1982) A thermochemical study of glasses and crystals along the joins silica-calcium aluminate and silica-sodium aluminate. Geochimica et Cosmochimica Acta, 46, 2039–2047.

N'Dala, I., Cambier, F., Anseau, M.R., and Urbain, G. (1984) Viscosity of liquid feldspars. I. Viscosity measurements. British Ceramic Transactions and Journal, 83, 105–107.

Ohtani, E., Taulelle, F., and Angell, C.A. (1985) Al^{3+} coordination changes in liquid aluminosilicates under pressure. Nature, 314, 78–81.

Okuno, M., and Marumo, F. (1982) The structures of anorthite and albite melts. Mineralogical Journal, 11, 180–196.

Press, W.H., Flannery, B.P., Teukolsky, S.A., and Vetterling, W.T. (1986) Numerical recipes: The art of scientific computing, 818 p. Cambridge University Press, New York.

Richet, P. (1984) Viscosity and configurational entropy of silicate melts. Geochimica et Cosmochimica Acta, 48, 471–483.

Richet, P., and Bottinga, Y. (1984) Glass transitions and thermodynamic properties of amorphous SiO_2, $NaAlSi_nO_{2n+2}$ and $KAlSi_3O_8$. Geochimica et Cosmochimica Acta, 48, 453–470.

Riebling, E.F. (1966) Structure of sodium aluminosilicate melts containing at least 50 mole % SiO_2 at 1500° C. The Journal of Chemical Physics, 44, 2857–2865.

Rivers, M.L., and Carmichael, I.S.E. (1987) Ultrasonic studies of silicate melts. Journal of Geophysical Research, 92(B), 9247–9270.

Roselieb, K., Rammensee, W., Buttner, H., and Rosenhauer, M. (1992) Solubility and diffusion of noble gases in vitreous albite. Chemical Geology, 96, 241–266.

Rustad, J.R., Yuen, D.A., and Spera, F.J. (1991a) Molecular dynamics of amorphous silica at very high pressures (135 GPa): Thermodynamics and extraction of structures through analysis of Voronoi polyhedra. Physical Review B, 44, 2108–2121.

———(1991b) The statistical geometry of amorphous silica at lower mantle pressures: Implications for melting slopes of silicates and anharmonicity. Journal of Geophysical Research, 96(B), 19665–19673.

———(1992) Coordination variability and the structural components of silica glass under high pressures. Chemical Geology, 96, 421–437.

Ryerson, F.J., Weed, H.C., and Piwinskii, A.J. (1988) Rheology of subliquidus magmas. I. Picritic compositions. Journal of Geophysical Research, 93(B), 3421–3436.

Scamehorn, C.A., and Angell, C.A. (1991) Viscosity-temperature relations and structure in fully polymerized aluminosilicate melts from ion dynamics simulations. Geochimica et Cosmochimica Acta, 55, 721–730.

Scarfe, C.M., and Cronin, D.J. (1986) Viscosity-temperature relationships

of melts at 1 atm in the system diopside-albite. American Mineralogist, 71, 767–771.

Scarfe, C.M., Mysen, B.O., and Virgo, D. (1987) Pressure dependence of the viscosity of silicate melts. In B.O. Mysen, Ed., Magmatic processes: Physicochemical principles, p. 59–67. The Geochemical Society, University Park, Pennsylvania.

Schairer, J.F., and Bowen, N.L. (1956) The system $Na_2O-Al_2O_3-SiO_2$. American Journal of Science, 254, 129–195.

Seifert, F.A., Mysen, B.O., and Virgo, D. (1982) Three-dimensional network structure of quenched melts (glass) in the systems $SiO_2-NaAlO_2$, $SiO_2-CaAl_2O_4$ and $SiO_2-MgAl_2O_4$. American Mineralogist, 67, 696–717.

Sharma, S.K., Virgo, D., and Mysen, B.O. (1978) Structure of melts along the join $SiO_2-NaAlSiO_4$ by Raman spectroscopy. Carnegie Institution of Washington Year Book, 77, 652–658.

——— (1979) Raman study of the coordination of aluminum in jadeite melts as a function of pressure. American Mineralogist, 64, 779–787.

Shaw, H.R. (1972) Viscosities of magmatic silicate liquids: An empirical method of prediction. American Journal of Science, 272, 870–893.

Spera, F.J., Borgia, A., Strimple, J., and Feigenson, M. (1988) Rheology of melts and magmatic suspensions. I. Design and calibration of concentric cylinder viscometer with application to rhyolitic magma. Journal of Geophysical Research, 93(B), 10273–10294.

Stein, D.J., and Spera, F.J. (1992) Rheology and microstructure of magmatic emulsions: Theory and experiments. Journal of Volcanology and Geothermal Research, 49, 157–174.

Stein, D.J., Spera, F.J., Rustad, J.R., and Yuen, D.A. (1992a) Viscosimetry and computer simulation studies of composition, structure and dynamics of sodium aluminosilicates in the system $SiO_2-NaAlSiO_4$ (abs.). Eos, 73 (Supplement), 356.

——— (1992b) Thermodynamic and transport properties of melts in the system $SiO_2-NaAlSiO_4$ by molecular dynamics simulations (abs.). Eos, 73 (Supplement), 356.

Taylor, M., and Brown, G.E., Jr. (1979a) Structure of mineral glasses. I. The feldspar glasses $NaAlSi_3O_8$, $KAlSi_3O_8$, $CaAl_2Si_2O_8$. Geochimica et Cosmochimica Acta, 43, 61–75.

——— (1979b) Structure of mineral glasses. II. The $SiO_2-NaAlSiO_4$ join. Geochimica et Cosmochimica Acta, 43, 1467–1473.

Taylor, M., Brown, G.E., Jr., and Fenn, P.M. (1980) Structure of mineral glasses. III. $NaAlSi_3O_8$ supercooled liquid at 805° C and the effects of thermal history. Geochimica et Cosmochimica Acta, 44, 109–117.

Taylor, T.D., and Rindone, G.E. (1970) Properties of aluminosilicate glasses. V. Low-temperature viscosities. American Ceramic Society Journal, 53, 692–695.

Urbain, G., Bottinga, Y., and Richet, P. (1982) Viscosity of liquid silica, silicates and alumino-silicates. Geochimica et Cosmochimica Acta, 46, 1061–1072.

Webb, S.L., and Dingwell, D.B. (1990) The onset of non-Newtonian rheology of silicate melts. A fiber elongation study. Physics and Chemistry of Minerals, 17, 125–132.

Zachariasen, W.H. (1932) The atomic arrangement in glasses. Journal of the American Chemical Society, 54, 3841–3851.

Ziman, J.M. (1979) Models of disorder, 525 p. Cambridge University Press, New York.